# Supporting Information

## Connaris et al. 10.1073/pnas.1404205111

### SI Materials and Methods

**Virus.** For in vitro studies, the following influenza viruses propagated in Madin–Darby canine kidney cells (MDCK) (American Type Culture Collection) were used: A/WSN/1933 (H1N1), A/Puerto Rico/8/1934 (A/PR/8/1934, H1N1), A/Udorn/1972 (H3N2), and B/Hong Kong/1973. Virus infectivity in MDCK cells was determined by plaque assay and expressed as $\log_{10}$pfu/mL. For in vivo studies, two strains were used: mouse-adapted A/WSN/1933 (H1N1) strain that was propagated in MDCK cells and mouse-adapted A/California/04/2009 (H1N1) virus (1) that was grown in embryonated chicken eggs. To determine the 50% mouse lethal dose ($MLD_{50}$) for A/California/04/2009 (H1N1), four female 6-wk-old BALB/c mice (Jackson Laboratories) were lightly anesthetized with isofluorane and intranasally inoculated with 50 μL of 10-fold serial dilutions of virus in PBS. The $MLD_{50}$ value was determined after a 21-d observation period.

**Generation of Multivalent Carbohydrate-Binding Modules.** The tandem-repeat multivalent protein *Vibrio cholerae* carbohydrate-binding module (*Vc*4CBM), based on the Family 40 (2) sialic acid-binding domain of the *nanH* gene encoding the sialidase from *V. cholerae,* was generated using PCR-based cloning techniques as described previously (3). Oligomerization of the CBM domain from *V. cholerae* nanH sialidase and from *Streptococcus pneumoniae* nanA sialidase, using the trimerization domain from the pseudaminidase protein from *Pseudomonas aeruginosa*, was engineered as follows: The DNA fragments encoding the CBM of *V. cholerae* sialidase (*Vc*CBM) (residues 25–216) and that of *S. pneumoniae* nanA sialidase (*Sp*CBM) (residues 121–305) were modified at the 5′ and 3′ termini by PCR amplification using primer pairs (Table S1) to incorporate different restriction sites to link one or two copies of the CBM unit in tandem for subsequent ligation to the gene encoding the trimerization domain (TD) from *P. aeruginosa* pseudaminidase (residues 333–438) (*Pa*TD). The resulting fragments were cloned either into an appropriately digested pEHISTEV vector (for *Vc*CBM) or a pEGFP-HISTEV vector (for *Sp*CBM) to create constructs designated as *Vc*CBMTD, *Vc*2CBMTD, *Sp*CBMTD, and *Sp*2CBMTD, respectively (Fig. 1*D*). The pEGFP-HISTEV vector also was used to create GFP-*Sp*CBM for glycan array studies and GFP-*Vc*2CBMTD and GFP-*Sp*2CBMTD for imaging studies. All constructs were propagated in *Escherichia coli* DH5a cells, and constructs were verified by DNA sequencing, before transforming the expression host *E. coli* BL21 Gold (DE3) for protein production.

**Multivalent CBM Expression, Purification, and Characterization.** Expression of engineered multivalent CBMs (mCBMs) was performed as described previously (3) with some modifications. Briefly, *E. coli* cells containing either His-tagged *Vc*CBMs or GFP-His-tagged *Sp*CBMs were lysed in a buffer containing PBS, 0.3 M NaCl, and 10 mM imidazole with DNase (20 μg/mL) and protease (minus EDTA) inhibitor tablets (Roche). Clarified lysates were applied onto a HisTrap HP column, precharged with nickel (GE Healthcare) before elution of histidine-tagged CBMs using PBS containing 0.3 M NaCl and 250 mM imidazole. Removal of the tag, unless otherwise stated, was performed by digestion in situ with Tobacco etch virus (TEV) protease overnight before material was reapplied to the nickel column. All mCBM proteins were purified further using size-exclusion chromatography with a HiPrep 16/60 Sephacryl S200HR column (GE Healthcare) in PBS, and then either a Vivapure S Maxi H (*Vc*CBMs) or a Q Maxi H (*Sp*CBMs) column (Sartorius) was used to remove endotoxins. GFP-tagged proteins also were subjected to affinity chromatography and size-exclusion chromatography as described above. Protein yield was calculated to be between 15–70 mg/L depending on the mCBM. Proteins remained stable for several months when stored −80 °C. Protein purity and size were verified by 12% (wt/vol) SDS/PAGE and mass spectrometry. Binding of purified mCBMs to sialic acid was verified by surface plasmon resonance (Biacore T-100, University of Edinburgh) using a streptavidin-coated biosensor chip immobilized with a multivalent, biotinylated α-2,3-sialyllactose-polyacrylamide (Glycotech) (Table S2).

**Glycan Microarray.** The glycan-binding specificity of GFP-*Sp*CBM was analyzed using Glycan slide array v4.2 (Consortium for Functional Glycomics). GFP-*Sp*CBM (200 μg/mL) was prepared for analysis as described previously (3) but was modified to allow the use of an anti-GFP antibody to enhance the fluorescence signal of binding.

**Cell Protection Assay.** For cell protection assays, confluent MDCK monolayers (in DMEM, 0.5% FCS) were incubated with mCBMs [10 mg/mL, appropriately diluted in serum-free (SF) DMEM] at 37 °C for 1 h. Monolayers were rinsed with SF-DMEM before inoculation with ∼100–200 pfu of influenza virus [A/WSN/1933 (H1N1), A/PR/8/1934 (H1N1), A/Udorn/1972 (H3N2), or B/Hong Kong/1973] for 1 h at 37 °C before washing. Cells were overlaid with 1.2% (wt/vol) Avicel (FMC Biopolymer) in 10 mM Hepes (pH 7.4) in DMEM supplemented with 2 μg/mL *N*-acetylated trypsin. Plates were incubated at 37 °C for 2–3 d. Plaques were visualized by fixing monolayers in 4% (vol/vol) formaldehyde and staining with 0.1% crystal violet. The $EC_{50}$ values of mCBMs that protect 50% of cells from virus were calculated for each mCBM from dose–response curves.

**Viral Replication Inhibition Assay.** Confluent MDCK cells (96-well format) were used to assess the inhibition of influenza A virus replication by mCBMs. Cells were incubated with different mCBMs for 1 h at 37 °C, before washing and the addition of influenza A virus [A/WSN/1933 (H1N1), A/PR/8/1934 (H1N1), or A/Udorn/1972 (H3N2)], multiplicity of infection (MOI) 0.01 pfu per cell] to monolayers for 1 h. The virus inoculum was removed, and SF DMEM containing *N*-acetylated trypsin (2.5 μg/mL) was added to cells and incubated for a further 16–24 h. Cells were fixed with 4% (vol/vol) formaldehyde and were permeabilized with PBS containing 0.5% Triton-X100 and 20 mM glycine (PBS-T) for 30 min before blocking with PBS containing 1% BSA, 0.02% sodium azide (BB), for 2–3 h. Cells were rinsed before the addition of goat anti-influenza A (1:500 dilution in BB; Santa Cruz) for 1–2 h at 22 °C. Plates were washed before the addition of donkey anti-goat IgG HRP-conjugated antibody (1:500 dilution; Santa Cruz). For color development, plates were incubated with 3,3′,5,5′′-tetramethylbenzidine (TMB; HRP substrate; Sigma). The reaction was stopped by the addition of 1 M HCl. Absorbance was measured at the 450-nm wavelength (620 nm was used as reference). $EC_{50}$ values were calculated from dose–response curves to determine the concentration of mCBM that inhibited 50% of viral replication compared with control (untreated, infected) wells.

**Cytotoxicity Assay.** The influence of mCBMs on the viability of mammalian epithelial (MDCK) cells during a 24-h period was evaluated using the PrestoBlue cell viability assay as described by the manufacturer (Life Technologies, Invitrogen). mCBMs (dilution of 5 mg/mL stock concentration) were added to confluent cell monolayers and incubated for 24 h at 37 °C, alongside

controls [DMEM only, untreated control, and 20% (wt/vol) sodium azide as positive control]. PrestoBlue reagent was added to cells and incubated for 1 h before absorbance was measured at the 570-nm wavelength (620 nm was used as reference). The relative absorbance of treated cells was expressed as a percentage of untreated cells plotted against the mCBM concentration. The concentration of mCBM required to reduce cell viability by 50% ($CC_{50}$) was determined from dose–response curves using a nonlinear regression curve fit with a variable slope.

**Imaging Studies.** To determine binding of mCBMs to sialylated epithelial cell surfaces, MDCK and human lung carcinoma (A549) cells were used. Cells were diluted to $3 \times 10^5$ cells/mL in DMEM supplemented with 10% (vol/vol) FCS before 100 μL was added to each well of a 96-well, black, flat-bottomed plate (Costar) or 1.5 mL was added to 35 × 10 mm glass-bottomed WillCo-dishes (WillCo Wells B.V). Cells were incubated overnight to 90–100% confluence. Cells were rinsed three times with warmed, sterile PBS, and the catalytic domain (residues 319–822) of the *S. pneumoniae* NanA sialidase (4) was added to cells at a concentration of 250 μg/mL in SF-DMEM and left to incubate for 1 h at 37 °C, 5% $CO_2$. Cells were rinsed extensively with PBS before addition of mCBM (0.05 mg/mL *Vc*2CBMTD or 0.1 mg/mL *Sp*2CBMTD in SF-DMEM) and were incubated further for 1 h at 37 °C, 5% $CO_2$. Cells were rinsed before rabbit polyclonal anti-mCBM antibody (Eurogentec) was added (1:1,000 in DMEM-3% FCS) and then were incubated for 1 h at 37 °C, 5% $CO_2$. This incubation was followed by the addition of goat anti-rabbit Alexa Fluor 488 IgG (Life Technologies) at 2 μg/mL in DMEM-3% FCS and further incubated for 1 h at 37 °C, 5% $CO_2$. Then DAPI was added for 30 min before a final washing of cells with PBS. Plates were read on a TECAN Infinite Pro-200 Fluorescence plate reader (using excitation and emission wavelengths of 488 nm and 530 nm, respectively). Live cells were imaged using a DeltaVision deconvolution microscope (Applied Precision) fitted with an Olympus IX71 camera, using excitation and emission wavelengths of 485 nm and 531 nm, respectively. To demonstrate mCBM blocking of influenza virus in mammalian cells, MDCK cells were prepared on coverslips in six-well plates to achieve 80–90% confluency and were incubated with GFP-Sp2CBMTD (0.1 mg/mL) or GFP-Vc2CBMTD (0.05 mg/mL) for 30–60 min at 37 °C, 5% $CO_2$. Cells were chilled for 30 min on ice before influenza A/WSN/1933 (H1N1), MOI of 5, was added for a further 30 min at the same temperature. Virus was removed by aspiration, and cells were transferred to 37 °C to incubate for a further 30–60 min before being fixed with 4% (vol/vol) paraformaldehyde and permeabilized with 0.1% (vol/vol) Triton-X 100 in PBS. Primary staining of virus was achieved using mouse monoclonal anti-influenza A NP antibody in 5% (vol/vol) horse serum-PBS (1:50 dilution; Santa Cruz Biotechnology) followed by Alexa Fluor 647-labeled anti-mouse IgG (1:1,000 dilution in 5% (vol/vol) horse serum-PBS; Life Technologies). Coverslips were mounted using ProLong Gold Antifade Reagent with DAPI (Life Technologies) and were imaged using the DeltaVision microscope as described above.

**Mice Infection Studies.** In vivo studies were conducted at The Roslin Institute (Edinburgh) and St. Jude Children's Research Hospital (Memphis, TN). Female BALB/c mice were purchased from Harlan Ltd (5- to 6-wk-old mice) or from Jackson Laboratories (6- to 8-wk-old mice). Studies in the United Kingdom were conducted at the animal testing facility for influenza research at the Centre for Infectious Diseases, Edinburgh, and were carried out under a UK Home Office License according to the Animals (Scientific Procedures) Act 1986. Mice were anesthetized using isoflurane (Rhone Merieux Ltd) before varying amounts of mCBM (50–500 μg in PBS) were administered intranasally either 24 h before or on the day of lethal viral challenge with $5 \times 10^3$ pfu of influenza A/WSN/1933 (H1N1) virus in 40 μL of PBS. Mice were weighed daily and assessed for visual signs of clinical disease. Animals that had lost 25% of their original body weight were culled by $CO_2$ asphyxiation. On day 7 post infection (p.i.), unless otherwise indicated, lungs were removed and were prepared as clarified tissue homogenates in PBS for cytokine/chemokine levels and viral load analysis using a standard plaque assay, as above, or were left whole for immunohistology.

Experiments with mouse-adapted A/California/04/2009 (H1N1) influenza virus were conducted in animal biosafety level 2+ containment approved for use by the US Department of Agriculture. All studies were conducted under applicable laws and guidelines and after approval by the St. Jude Children's Research Hospital Animal Care and Use Committee. Groups of BALB/c mice ($n$ = 5) were given 50 μL of mCBMs intranasally with a single, double, or triple dose ranging from 0.1–500 μg per mouse unless specified otherwise. Treatment with mCBMs protein was initiated at different time points between day −7 and day +1 of viral challenge. Animals were inoculated with A/California/04/2009 (H1N1) influenza virus at a dose of 10 $MLD_{50}$ (150 pfu) per mouse. Control (infected, untreated) mice received 50 μL of sterile PBS intranasally 1 h before virus inoculation. mCBM toxicity controls (uninfected, treated mice) were tested also. Mice were observed daily for 21 d p.i. for clinical signs of infection and survival, and weight was recorded throughout the infection period. Virus lung titers were determined on days 3, 6, and 9 p.i. in additional groups of mice ($n$ = 3) by a 50% tissue culture infectious dose ($TCID_{50}$) assay in MDCK cells.

**Immunohistology.** Lungs of mice were inflated and fixed with 10% (vol/vol) neutral buffered formalin (Surgipath, Leica Systems) before being embedded in paraffin wax. For immunofluorescence, tissue sections were cut and stained for *Sp*2CBMTD using polyclonal anti-*Sp*CBM sera raised in rabbit (1:1,000 dilution; Eurogentec) followed by goat anti-rabbit IgG Alexa Fluor 488 secondary antibody (1:4,000; Invitrogen) in CAS-Block reagent (Invitrogen). For primary antibody control, rabbit IgG isotype control serum (Gene Tex) was used. Slide sections were mounted in ProLong Gold Antifade Reagent with DAPI (Life Technologies) before tissue was imaged with a Leica DMRB microscope fitted with a Leica DFC 300 FX.

**Cytokine Analysis.** Cytokine analyses of clarified mouse lung homogenates were performed using Quantikine ELISA kits (RD Biosystems) according to the manufacturer's instructions.

**Antibody Analysis.** Immune sera collected from survived mice 21 d p.i. were tested for both anti-viral HA antibodies and for the presence of anti-mCBM antibodies. HA inhibition assays were performed with 0.5% packed chicken red blood cells on sera that were pretreated with receptor-destroying enzyme (RDE II; 1:10 dilution; Denka Seiken Co.) and were heat inactivated at 56 °C for 30 min. A standard ELISA was used to measure anti-CBM antibodies from infected mouse sera samples using prepared antigens (1 μg per well) immobilized on 96-well plates (Corning). Sera (diluted 1:1,000 in BB) were added to wells followed by goat anti-mouse IgG, IgA, or IgM HRP-conjugate antibodies (1:2,500 dilution), and the presence of antibodies was detected using TMB as described above. To test for preexisting immunity of sialic acid-binding CBMs in the human population, human sera samples ($n$ = 50) obtained from a mixed aged population of males and females (Seralab) were used. Sera were diluted 1:1,000, before a standard ELISA was applied to test for anti-*Vc*CBM and anti-*Sp*CBM antibodies using goat anti-human IgG-conjugated HRP (1:2,500).

**Statistical Analysis.** For survival studies, the Kaplan–Meier method was used to estimate the probability of survival of

untreated and treatment groups. Data plotted with error bars are expressed as means ± SD unless otherwise indicated. Statistical significance ($P < 0.05$) between two groups was determined using the nonparametric Mann–Whitney $u$ test. GraphPad Prism 5.0 package (GraphPad Software Inc.) was used for all analysis.

1. Ilyushina NA, et al. (2010) Adaptation of pandemic H1N1 influenza viruses in mice. *J Virol* 84(17):8607–8616.
2. Cantarel BL, et al. (2009) The Carbohydrate-Active EnZymes database (CAZy): an expert resource for Glycogenomics. *Nucleic Acids Res* 37(Database issue):D233–D238.
3. Connaris H, Crocker PR, Taylor GL (2009) Enhancing the receptor affinity of the sialic acid-binding domain of *Vibrio cholerae* sialidase through multivalency. *J Biol Chem* 284(11):7339–7351.
4. Xu G, Li X, Andrew PW, Taylor GL (2008) Structure of the catalytic domain of *Streptococcus pneumoniae* sialidase NanA. *Acta Crystallogr Sect F Struct Biol Cryst Commun* 64(Pt 9):772–775.

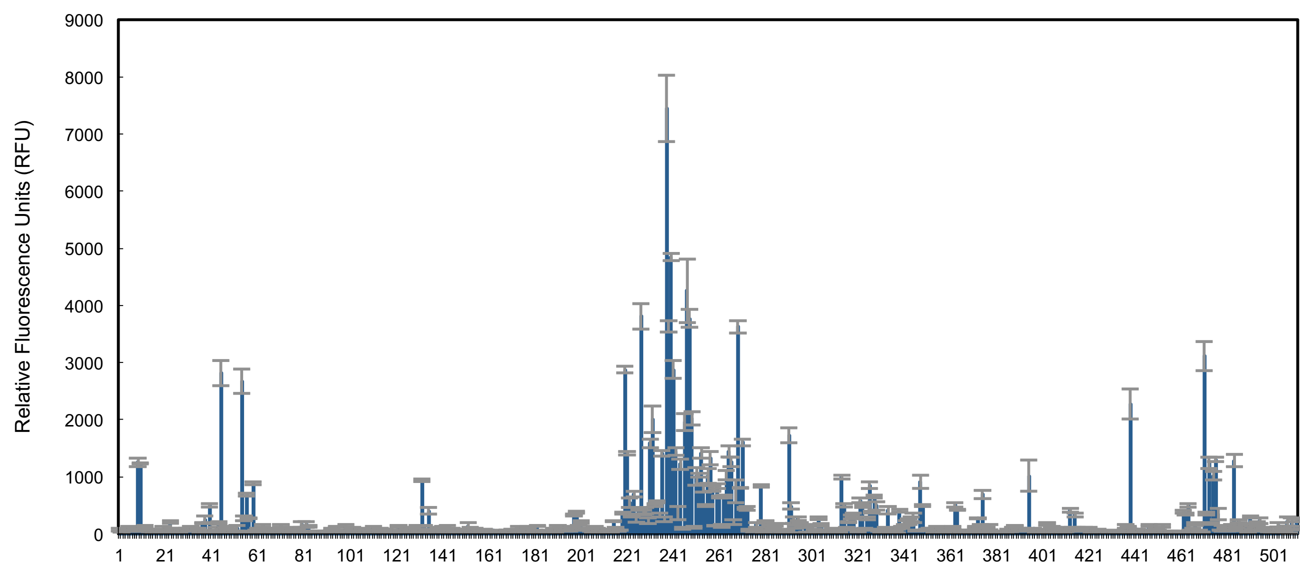


| Glycan Number | Glycan Structure | Avg RFU | StDev | SEM | %CV |
|---|---|---|---|---|---|
| 238 | Neu5Acα2-3Galβ1-3(Neu5Acα2-3Galβ1-4)GlcNAcβ-Sp8 | 7447 | 1170 | 585 | 16 |
| 240 | Neu5Acα2-3Galβ1-3(Neu5Acα2-6)GalNAcα-Sp8 | 4850 | 134 | 67 | 3 |
| 247 | Neu5Acα2-3Galβ1-3GlcNAcβ-Sp8 | 4255 | 1124 | 562 | 26 |
| 227 | Neu5Acα2-3(6-O-Su)Galβ1-4(Fucα1-3)GlcNAcβ-Sp8 | 3809 | 450 | 225 | 12 |
| 248 | Neu5Acα2-3Galβ1-4[6OSO3]GlcNAcβ-Sp8 | 3771 | 309 | 155 | 8 |
| 239 | Neu5Acα2-3Galβ1-3[6OSO3]GalNAcα-Sp8 | 3636 | 206 | 103 | 6 |
| 269 | Neu5Acα2-6Galβ1-4Glcβ-Sp0 | 3624 | 222 | 111 | 6 |
| 471 | Neu5Acα2-3Galβ1-4GlcNAcβ1-2Manα-Sp0 | 3114 | 515 | 258 | 17 |
| 241 | Neu5Acα2-3Galβ1-3(Neu5Acα2-6)GalNAcα-Sp14 | 2875 | 306 | 153 | 11 |
| 220 | Neu5Acα2-3Galβ1-3GalNAcα-Sp8 | 2875 | 129 | 65 | 4 |
| 45 | Neu5Acα2-3[6OSO3]Galβ1-4GlcNAcβ-Sp8 | 2816 | 445 | 223 | 16 |
| 54 | Neu5Acα2-6Galβ1-4GlcNAcβ1-2Manα1-3(Neu5Acα2-6Galβ1-4GlcNAcβ1-2Manα1-6)Manβ1-4GlcNAcβ1-4GlcNAcβ-N(LT)AVL | 2673 | 427 | 214 | 16 |
| 439 | Neu5Acα2-3Galβ1-4GlcNAcβ1-3Galβ-Sp8 | 2270 | 518 | 259 | 23 |
| 249 | Neu5Acα2-3Galβ1-4(Fucα1-3)[6OSO3]GlcNAcβ-Sp8 | 2024 | 239 | 120 | 12 |
| 232 | Neu5Acα2-3(Neu5Acα2-6)GalNAcα-Sp8 | 2001 | 461 | 231 | 23 |
| 246 | Neu5Acα2-3Galβ1-3GlcNAcβ-Sp0 | 1958 | 300 | 150 | 15 |
| 291 | Neu5Acα2-3Galβ1-3GlcNAcβ1-3Galβ1-3GlcNAcβ-Sp0 | 1729 | 269 | 134 | 16 |
| 271 | Neu5Acα2-6Galβ-Sp8 | 1601 | 124 | 62 | 8 |
| 231 | Neu5Acα2-3(Neu5Acα2-3Galβ1-3GalNAcβ1-4)Galβ1-4Glcβ-Sp0 | 1584 | 161 | 80 | 10 |
| 265 | Neu5Acα2-6Galβ1-4GlcNAcβ-Sp0 | 1443 | 195 | 97 | 13 |
| 242 | Neu5Acα2-3Galβ-Sp8 | 1439 | 145 | 72 | 10 |
| 253 | Neu5Acα2-3Galβ1-4(Fucα1-3)GlcNAcβ1-3Galβ-Sp8 | 1415 | 191 | 96 | 14 |
| 221 | Neu5Acα2-3Galβ1-3GalNAcα-Sp14 | 1413 | 65 | 32 | 5 |
| 236 | Neu5Acα2-3Galβ1-3(Fucα1-4)GlcNAcβ-Sp8 | 1409 | 97 | 48 | 7 |
| 257 | Neu5Acα2-3Galβ1-4GlcNAcβ-Sp8 | 1326 | 243 | 121 | 18 |
| 476 | Neu5Acα2-3Galβ1-4GlcNAcβ1-2Manα1-6(Neu5Acα2-3Galβ1-4GlcNAcβ1-2Manα1-3)Manβ1-4GlcNAcβ1-4(Fucα1-6)GlcNAcβ-6AA | 1300 | 69 | 34 | 5 |
| 484 | Neu5Acα2-3Galβ1-3GlcNAcβ1-6GalNAcα-Sp14 | 1282 | 220 | 110 | 17 |
| 266 | Neu5Acα2-6Galβ1-4GlcNAcβ-Sp8 | 1258 | 164 | 82 | 13 |
| 9 | Neu5Acα-Sp8 | 1252 | 151 | 75 | 12 |

**Fig. S1.** (*Upper*) Glycan array screen for *Sp*CBM showing its specificity and promiscuity for terminal sialic acid glycans. Glycan binding of GFP-fused *Sp*CBM, using glycan array v4.2 consisting of 511 glycans (Consortium for Functional Glycomics), is expressed as relative fluorescence units (RFU). The top 40 hits are all sialosides. (*Lower*) Only the first 29 glycans are listed in decreasing order of RFU. Error bars indicate the SEM in the signal for four independent replicates. Confidence value (%CV) = 100 × SD/mean RFU.

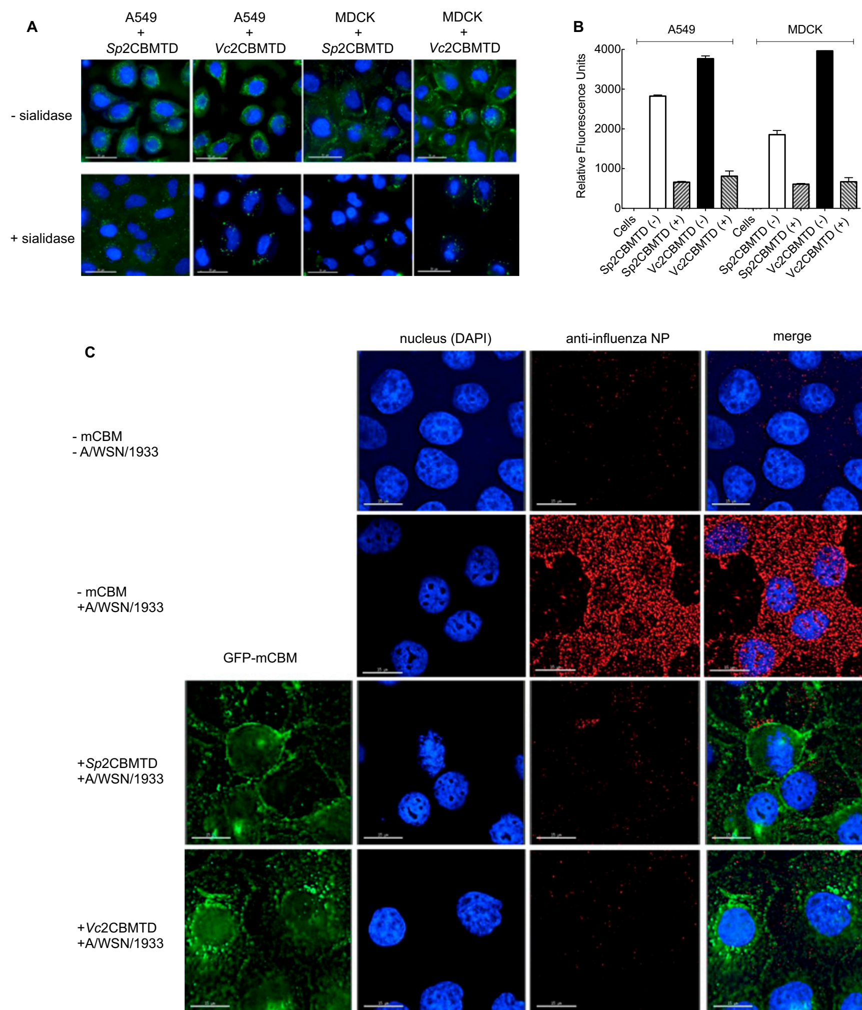


**Fig. S2.** Cell-surface binding and efficacy of *Sp*2CBMTD and *Vc*2CBMTD in preventing viral attachment. (*A*) Representation of live images of A549 and MDCK cells showing *Sp*2CBMTD and *Vc*2CBMTD binding before (*Upper Row*) and after treatment with the catalytic domain of *S. pneumoniae* NanA sialidase (*Lower Row*). mCBMs were stained using rabbit anti-*Sp*CBM and anti-*Vc*CBM antibodies, respectively, before incubation with Alexa Fluor 488-labeled anti-rabbit IgG antibody. Nuclei are stained using DAPI (blue). (Scale bars, 30 μm.) (*B*) Relative fluorescence units (RFU) of mCBM binding to cells when treated with or without sialidase. Bars represent means ± SD. for each treated and untreated groups. (*C*) Fluorescent images of MDCK cells preincubated with or without GFP-*Sp*2CBMTD or GFP-*Vc*2CBMTD followed by incubation with influenza A/WSN/1933 (MOI= 5). Cells were fixed and incubated with mouse anti-influenza A virus NP antibody before staining with Alexa Fluor 647-labeled anti-mouse antibody. Nuclei were stained with DAPI during the mounting of tissues with ProLong Gold Anti-Fade reagent. (Scale bars 15 μm.)

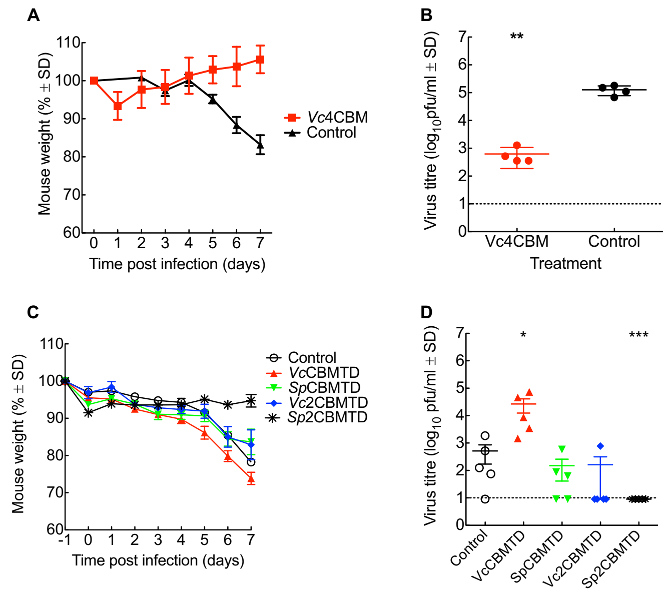


**Fig. S3.** Weight changes and lung viral titers of BALB/c mice after lethal challenge with A/WSN/1933 (H1N1) influenza virus. (*A*) Weight changes in mice ($n = 4$) after a single intranasal administration of 500 μg of *Vc*4CBM or PBS (control) immediately before viral challenge. (*B*) Lung viral titers in mice determined 7 d p.i. (*C*) Weight changes in mice ($n = 4$) after a single intranasal administration of a trimeric (*Vc*CBMTD, *Sp*CBMTD, 400 μg) or hexameric (*Vc2*CBMTD, *Sp2*CBMTD, 100 μg) biologic or PBS (control), immediately before viral challenge. (*D*) Lung virus titers in mice determined 7 d p.i. The dashed line indicates the limit of virus detection. Bars represent means ± SD for each treated and control group. $*P < 0.05$, $**P < 0.001$, $***P < 0.0001$.

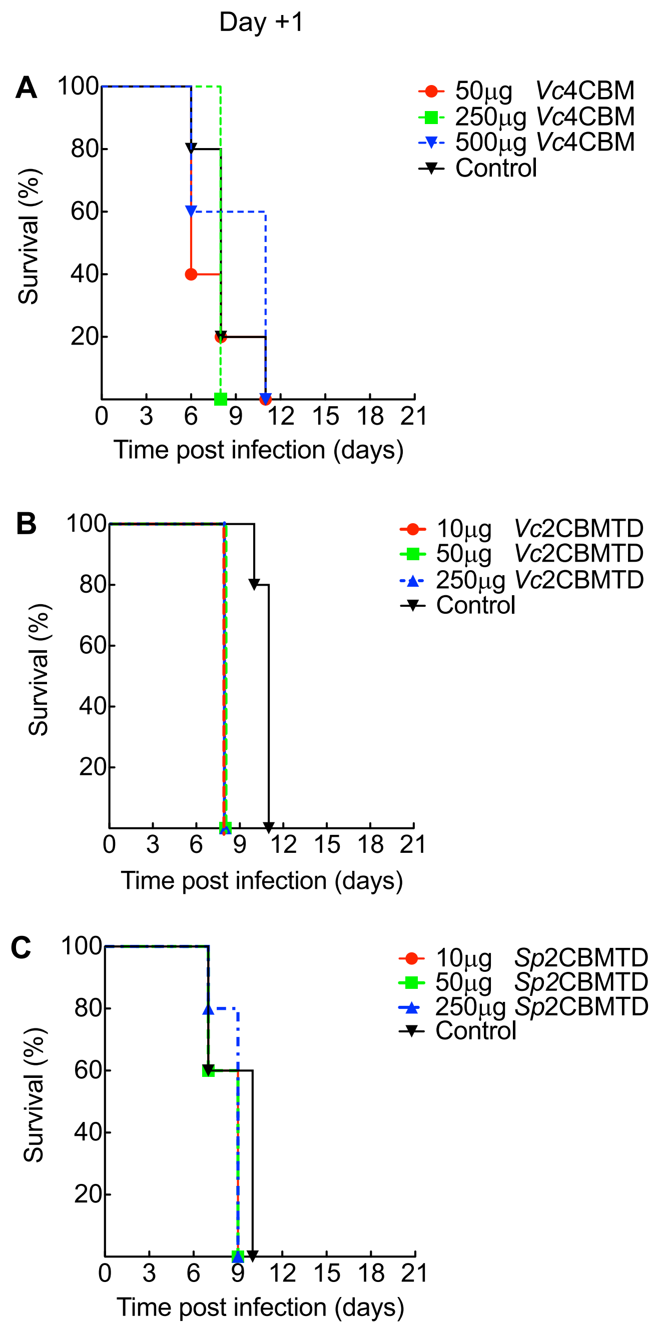


**Fig. S4.** Survival of BALB/c mice administered with mCBMs 24 h after challenge with mouse-adapted A/California/04/2009 (H1N1) influenza virus. BALB/c mice ($n = 5$) were administered a single dose of *Vc*4CBM (*A*), *Vc*2CBMTD (*B*), or *Sp*2CBMTD (*C*) intranasally 1 d after viral challenge and were monitored for survival. Graphs represent the survival curves with different doses of each mCBM.

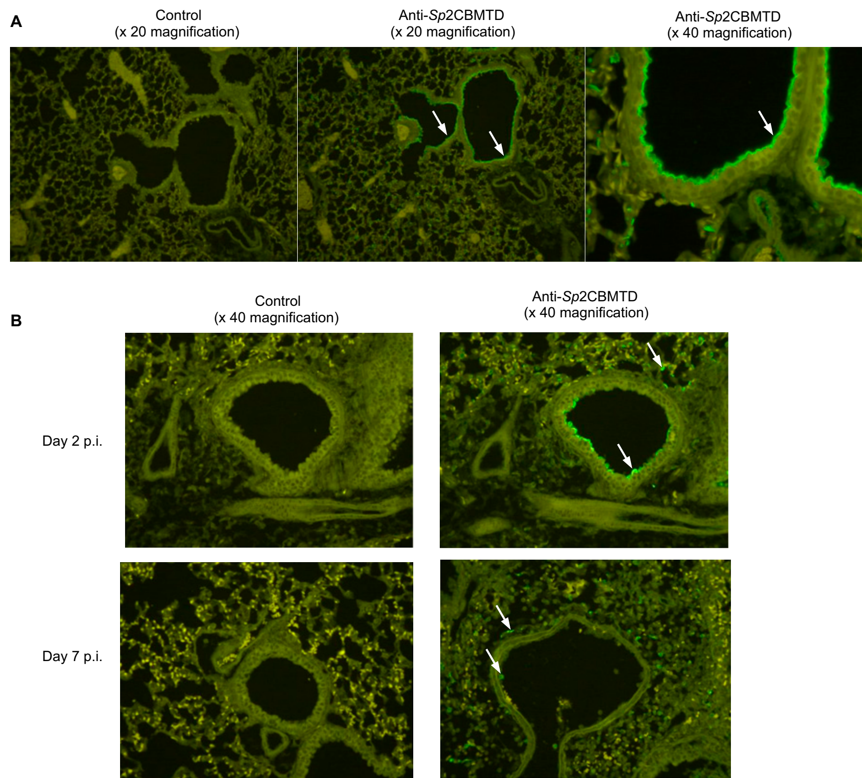


**Fig. S5.** Images of uninfected and A/WSN/1933 (H1N1) influenza virus-infected mouse lung tissues when treated with *Sp*2CBMTD. Fluorescent images showing the presence of the biologic in lung were identified using rabbit anti-*Sp*CBM and Alexa Fluor 488-labeled anti-rabbit IgG antibodies. (*A*) Images of uninfected mouse lung tissues 1 d after intranasal administration of a single dose of *Sp*2CBMTD (400 μg). (*B*) Images of influenza A/WSN (H1N1) virus-infected mouse lung tissues after administration of a single dose of *Sp*2CBMTD (50 μg) 1 d before a lethal virus challenge. Mouse lungs were harvested at days 2 and 7 p.i. For control tissue staining, rabbit IgG isotype control serum was used. White arrows indicate the location of *Sp*2CBMTD on alveoli epithelial cell surfaces.

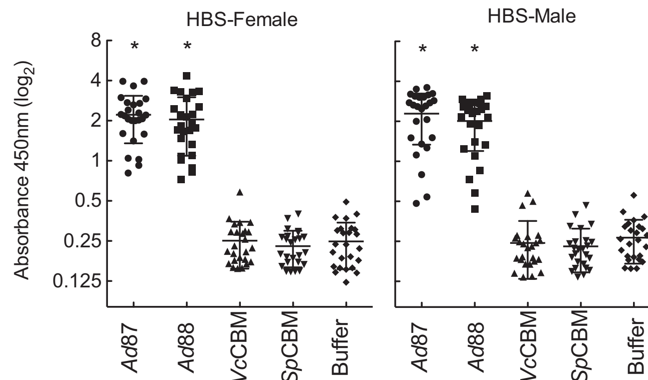


**Fig. S6.** Demonstration of the absence of preexisting immunity to *Vc*CBM or *Sp*CBM in the human population. Human blood sera were analyzed for the presence of anti-CBM antibodies using ELISA. Samples ($n = 50$) were obtained from a mixed-age population of males and females (Seralab). *Ad*87 and *Ad*88 are positive controls for adenovirus antibodies. Error bars represent SD as measured against buffer block (no serum). *$P < 0.001$.

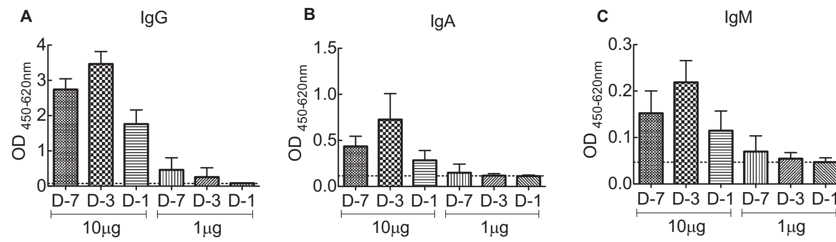


**Fig. S7.** Detection of sera IgA, IgG, and IgM antibodies to *Sp2*CBMTD after treatment in mice. Mice were administered 10 or 1 µg (50 µL) of *Sp*2CBMTD intranasally on day −7, −3, or −1 before challenge with mouse-adapted A/California/04/2009 (H1N1) influenza virus on day 0. Sera were taken on day 21 p.i. to assess anti-*Sp*2CBMTD antibodies by ELISA, as described in *SI Materials and Methods*. Bars indicate the mean absorbance change ± SD for IgG (*A*), IgA (*B*), and IgM (*C*) from three mice per group. The dashed line indicates the limit of detection of assay for IgG ($A_{450\text{–}620nm}$ 0.074), IgA (0.115), and IgM (0.047).

**Table S1. Primers used for engineering the mCBMs**

| | Features | Primers | Linker sequences |
|---|---|---|---|
| *Vc*CBMTD | NcoI-*Vc*CBM-BamHI-*Pa*TD-Stop-XhoI | VcCBMNcoI(F) 5′–GGCT**CCATGG**CACTTTTTGACTATAACGC–3′<br>VcCBMBamHI(R)5′–GCAC**GGATCC**ACCACCGTCGCCTTGAATTTC–3′<br>PaTDBamHI(F) 5′–GGCT**GGATCC**GGTATGGTCCCGGATTTTGAGTCA–3′<br>PaTDXhoI(R) 5′–CCGA**CTCGAG**CTAAATCCATGCTCTGACCCG–3′ | GGGSG |
| *Vc*2CBMTD | NcoI-*Vc*CBM-BamHI-*Vc*CBM-*Hind*III-*Pa*TD-Stop-XhoI | VcCBMNcoI(F) 5′–GGCT**CCATGG**CACTTTTTGACTATAACGC–3′<br>VcCBMBamHI(R) 5′–GCAC**GGATCC**ACCACCGTCGCCTTGAATTTC–3′<br>VcCBMBamHI(F) 5′–GGCT**GGATCC**GGTGCACTTTTTGACTATAAC–3′<br>VcCBMHindIII(R) 5′–GTCCCA**AAGCTT**GACCGTCGCCTTGAATTTC3–′<br>PaTDHindIII(F) 5′–CTGC**AAGCTT**TGGGAGTCCCGGATTTTGAGTCAG–3′<br>PaTDXhoI(R) 5′–CCGA**CTCGAG**CTAAATCCATGCTCTGACCCG–3′ | GGGSG and GQALG |
| *Sp*CBMTD | NcoI-*Sp*CBM-BamHI-*Pa*TD-Stop-XhoI | SpCBMNcoI(F) 5′–GGCT**CCATGG**TGATAGAAAAAGAAGATG–3′<br>SpCBMBamHI(R) 5′–ACC**GGATCC**ACCACCACTACGTTTTTGTACCTC–3′<br>PaTDBamHI(F) 5′–GGCT**GGATCC**GGTATGGTCCCGGATTTTGAGTCA–3′<br>PaTDXhoI(R) 5′–CCGA**CTCGAG**CTAAATCCATGCTCTGACCCG–3′ | GGGSG |
| *Sp*2CBMTD | NcoI-*Sp*CBM-BamHI-*Sp*CBM-*Hind*III-*Pa*TD-Stop-XhoI | SpCBMNcoI(F) 5′–GGCT**CCATGG**TGATAGAAAAAGAAGATG–3′<br>SpCBMBamHI(R) 5′–ACC**GGATCC**ACCACCACTACGTTTTTGTACCTC–3′<br>SpCBMBamHI(F) 5′–GGCT**GGATCC**GGTGTGATAGAAAAAGAAGATG–3′<br>SpCBMHindIII(R) 5′–TCCCA**AAGCTT**GACCACTACGTTTTTGTGCCTC–3′<br>PaTDHindIII(F) 5′–CTGC**AAGCTT**TGGGAGTCCCGGATTTTGAGTCAG–3′<br>PaTDXhoI(R) 5′–CCGA**CTCGAG**CTAAATCCATGCTCTGACCCG–3′ | GGGSG and GQALG |
| GFP-*Sp*CBM* | GFP-NcoI-*Sp*CBM Stop-XhoI | SpCBMNcoI(F) 5′–GGCT**CCATGG**TGATAGAAAAAGAAGATG–3′<br>SpCBMXhoI(R) 5′–GCA**CTCGAG**TCATTTAAAAAGTTGACTACGTTTTTGTAC–3′ | |

Restriction enzyme sites in primers are highlighted in bold.
*SpCBM gene fused in-frame with GFP gene using pEHISTEV-GFP vector as described in *SI Materials and Methods*.

**Table S2. Kinetic parameters for the different mCBMs interacting with multivalent α-2,3-sialyllactose**

| mCBM | Temperature, °C | $k_a$*, M/s | $k_d$†, s | $K_D$‡, nM |
|---|---|---|---|---|
| *Vc*4CBM | 15 | 0.54 ± 0.01 | 0.51 ± 0.01 | 0.94 |
| | 25 | 3.56 ± 0.02 | 1.60 ± 0.01 | 0.45 |
| | 37 | 2.98 ± 0.02 | 5.41 ± 0.04 | 1.82 |
| *Vc*CBMTD | 15 | 2.55 ± 0.02 | 4.20 ± 0.02 | 1.65 |
| | 25 | 7.24 ± 0.06 | 12.4 ± 0.10 | 1.71 |
| | 37 | 20.7 ± 0.54 | 107. ± 2.80 | 5.15 |
| *Vc*2CBMTD | 15 | 1.83 ± 0.01 | 0.33 ± 0.01 | 0.18 |
| | 25 | 1.73 ± 0.01 | 0.70 ± 0.01 | 0.41 |
| | 37 | 8.45 ± 0.05 | 2.07 ± 0.01 | 0.24 |
| *Sp*CBMTD | 15 | 0.73 ± 0.01 | 0.30 ± 0.01 | 0.41 |
| | 25 | 3.49 ± 0.02 | 1.37 ± 0.01 | 0.39 |
| | 37 | 1.95 ± 0.01 | 0.90 ± 0.01 | 0.46 |
| *Sp*2CBMTD | 15 | 0.03 ± 0.00 | 0.56 ± 0.04 | 17.25 |
| | 25 | 2.39 ± 0.01 | 1.35 ± 0.01 | 0.56 |
| | 37 | 0.70 ± 0.01 | 3.65 ± 0.04 | 5.21 |

Values for $k_a$ and $k_d$ are $\times 10^6$ and $\times 10^{-3}$, respectively.

*$k_a$ represents the association ("on") rate constant expressed as the mean ± SD of three replicates.

†$k_d$ represents the dissociation ("off'") rate constant expressed as the mean ± SD of three replicates.

‡$K_D$, represents the dissociation constant for each interaction between an mCBM and α-2,3-sialyllactose at three different temperatures, as determined by a global fit model (assuming Langmuir binding), derived from the ratio of $k_a/k_d$.

**Table S3. In vitro cell protection, inhibition of virus replication, and cell viability of the mCBMs**

| | Cell protection, $EC_{50}$*, μM | | | | | Therapeutic index‡ | | | | Viral replication inhibition, $EC_{50}$§, μM | | |
|---|---|---|---|---|---|---|---|---|---|---|---|---|
| mCBM | A/WSN/ H1N1 | A/PR8/ H1N1 | A/Udorn/ H3N2 | B/HK/73 | $CC_{50}$†, μM | A/WSN/ H1N1 | A/PR8/ H1N1 | A/Udorn/ H3N2 | B/HK/73 | A/WSN/ H1N1 | A/PR8/ H1N1 | A/Udorn/ H3N2 |
| *Vc*CBM | >300 | >300 | >300 | ND | ND | ND | ND | ND | ND | ND | ND | ND |
| *Vc*4CBM | 1.08 ± 0.01 | 1.43 ± 0.33 | 0.49 ± 0.01 | 1.97 ± 0.83 | >58.8 | >54 | >41 | >119 | >30 | 1.10 ± 0.03 | 4.80 ± 1.68 | 2.60 ± 1.60 |
| *Vc*CBMTD | 1.07 ± 0.43 | 2.75 ± 0.25 | 0.87 ± 0.32 | 3.95 ± 0.45 | >50 | >46 | >18 | >57 | >13 | 3.20 ± 0.50 | 10.75 ± 4.75 | 1.70 ± 0.02 |
| *Vc*2CBMTD | 0.39 ± 0.02 | 0.90 ± 0.03 | 0.47 ± 0.05 | 0.62 ± 0.08 | >30.5 | >79 | >34 | >65 | >49 | 0.50 ± 0.07 | 1.34 ± 0.65 | 0.45 ± 0.05 |
| *Sp*CBMTD | 1.11 ± 0.01 | 3.80 ± 0.03 | 0.82 ± 0.09 | 4.10 ± 0.10 | >50 | >43 | >13 | >61 | >12 | 4.25 ± 0.75 | 44.50 ± 0.50 | 5.70 ± 1.30 |
| *Sp*2CBMTD | 3.10 ± 0.40 | 1.85 ± 0.55 | 0.55 ± 0.15 | 2.80 ± 0.80 | >30.5 | >9 | >16 | >55 | >11 | 3.35 ± 0.65 | 10.00 ± 1.20 | 2.05 ± 0.95 |

ND, not determined because of the high concentrations of monomeric *Vc*CBM required for effective binding of cell-surface receptors.

*$EC_{50}$ is the concentration of mCBM that provides 50% cell protection, expressed as mean ± SD from three independent determinations.

†$CC_{50}$ values determined by the PrestoBlue cell viability assay as described in *SI Materials and Methods*, with > sign representing values using the maximum feasible concentration.

‡Therapeutic index is calculated from the ratio $CC_{50}$/*$EC_{50}$.

§$EC_{50}$ values determined by the concentration of mCBM that inhibits 50% viral replication expressed as mean ± SD from three independent determinations.